View metadata, citation and similar papers at core.ac.uk
brought to you by CORE
provided by Universidade do Minho: RepositoriUM

"Magnetic Gradient" edge magnetoplasmons in non-uniform magnetic field

O G Balev[1] and I A Larkin[2]

Abstract. It is shown that laterally inhomogeneous strong magnetic field applied to otherwise spatially homogeneous two-dimensional electron system (2DES) allows "magnetic gradient" or special magnetic-edge magnetoplasmons (MEMPs). This mechanism is different from usual "density gradient" edge magnetoplasmons. Symmetric and antisymmetric families of MEMPs are obtained. They are localized at magnetic field inhomogeneity (magnetic-edge). Both symmetric and antisymmetric MEMPs have the modes of opposite chirality.

[1] Departamento de Física, Universidade Federal do Amazonas, 69077-000, Manaus, AM, Brazil
[2] Department of Physics, Minho University, Braga 4710-057, Portugal

E-mail: ogbalev@ufam.edu.br
vaniala2000@yahoo.co.uk

Different types of "density gradient" edge magnetoplasmons (EMPs) have been studied for 2DES subjected to a strong homogeneos magnetic fiels [1, 2, 3, 4, 5]. These EMPs appear due to a strong change of the stationary local electron density at the edge of the channel (in particular, in the vicinity of edge states) that induces a strong modulation of the local magnetoconductivity tensor (modulation of the nondiagonal components is especially important), e.g., see [1, 3, 5]. Here we present theoretical study of the chiral modes in 2DES induced by "magnetic gradient". I.e., of special magnetic-edge magnetoplasmons (MEMPs) localized in a vicinity of magnetic field inhomogeneity. MEMPs are absent if a strong magnetic field applied to 2DES is homogeneous.

We consider homogeneous 2DES, localized within $z = 0$ plane, that is embedded in GaAs based sample, with the dielectric constant ε, that occupies a half-space $z < d$. In addition, 2DES is subjected to a strong laterally inhomogeneos magnetic field $\mathbf{B}(y) = B(y)\hat{\mathbf{z}}$, which appears due to ferromagnetic semi-infinite film of a finite thickness ηd. Fig. 1 presents a model geometry under discussion; the x-axis points out of the figure plane, and the y-axis points to the right from the ferromagnetic film. A finite external spatially homogeneous magnetic field $\mathbf{B}_{ext} = B_{ext}\hat{\mathbf{z}}$ is applied as well; $B_{ext} > 0$. We assume that the surface of heterostructure crystal, at $z = d$, has pined potential [6], or covered by a nonmagnetic-metallic gate. In addition, we assume that at $z = 0$ plane the ions jellium background of the constant area density n_I is located. Let us assume that magnetic field $B(y)$ is a smooth function of y, with the characteristic scale Δy. Comparing the pertubation of the electron density of 2DES, without metallic gates, due to spatially inhomogeneous magnetic field shows that even at the characteristic filling factor $\nu \leq 2$ the density of 2DES is very weakly modified if the Bohr radius $a_B \ll 2\Delta y$ and the quantum magnetic length $\ell_0(y) \ll 2\Delta y$; $\ell_0(y) = \sqrt{\hbar c/|e|B(y)}$. Below we assume that these conditions are satisfied and, respectively, the static electron density will be taken as n_I.

We assume that the low-frequency, $\omega \ll \omega_c$, and the long-wavelength, ($k_x\ell_0(y) \ll 1$ if $\nu \leq 2$), conditions are satisfied. Then the current density induced by a wave can be calculated in the

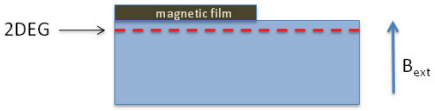

Figure 1. 2DES, at $z = 0$, is embedded in heterostructure, $z < d$. We assume pined potential at $z = d$, to ensure that one may cover the surface by metallic-nonmagnetic film (gate) Ferromagnetic semi-infinite film ($y < 0$, $d < z < d(1 + \eta)$) induces inhomogeneity of magnetic field.

quasi-static approximation [3, 5] as

$$j_x(y) = \sigma_{xx}(y)E_x(y) - \sigma^0_{yx}(y)E_y(y), \quad j_y(y) = \sigma_{yy}(y)E_y(y) + \sigma^0_{yx}(y)E_x(y), \tag{1}$$

where we have suppressed the exponential factor $\exp[-i(\omega t - k_x x)]$ and common arguments ω, k_x in $j_\mu(y)$, $E_\mu(y)$. Further, we will neglect by a dissipation assuming a clean 2DES and sufficiently low temperatures T.

For the setup of Fig. 1 with the constant magnetic moment of the ferromagnetic semi-infinite film along the $z-$axis, $\mathbf{M}_0 = M_0\hat{\mathbf{z}}$, readily it follows [7] that $B(y) = B_{ext} - 2M_0\{\arctan(Y) - \arctan(Y/(1+\eta))\}$, where $Y = y/d$. Assuming $\max\{|B(y) - B_{ext}|\} \ll B_{ext}$ we can approximate $1/B(Y)$ as

$$\frac{1}{B(y)} = \frac{1}{B_{ext}} - \frac{1}{2B_0}\{\arctan(Y/(1+\eta)) - \arctan(Y)\}, \tag{2}$$

where $B_0 = B^2_{ext}/(4M_0)$. From Eq. (2) it follows that $B(\pm\infty) = B_{ext}$. We assume that $B_0 > 0$.

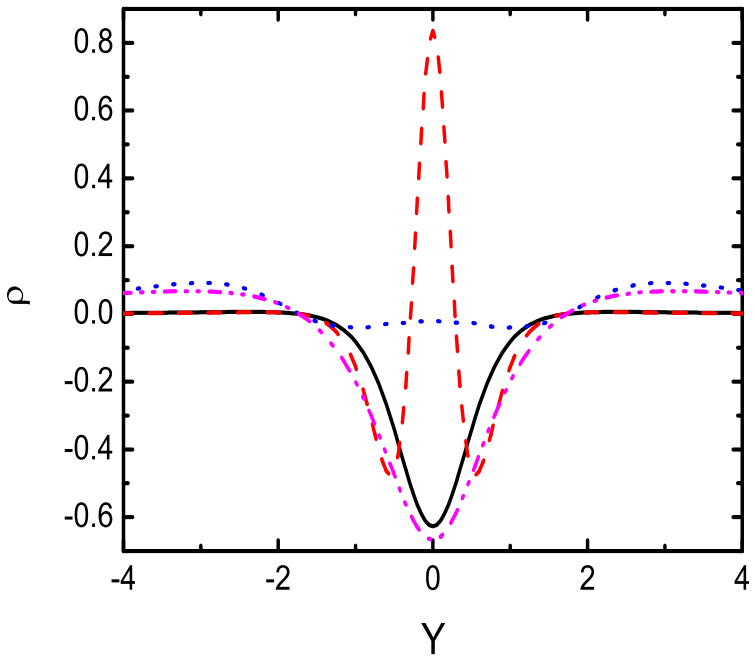

Figure 2. Spatial profile, at $\eta = 1$ and conditions of the table 1, for three fastest symmetric MEMPs W_{s1}, W_{s2}, and W_{s3} are plotted by the solid, the dashed, and the dotted curves. The dot-dot-dashed curve plots $g_0(Y)$.

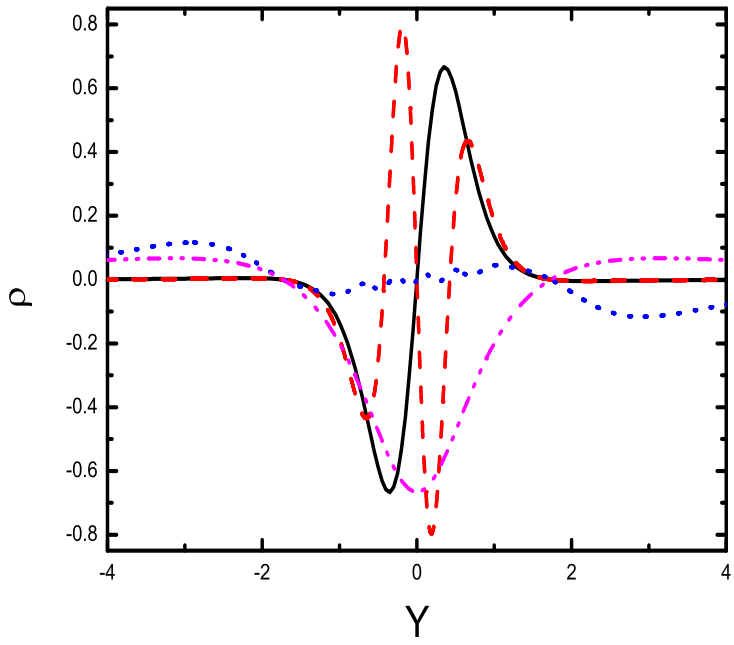

Figure 3. Spatial profile, at $\eta = 1$ and conditions of the table 1, for three fastest antisymmetric MEMPs W_{a1}, W_{a2}, and W_{a3} are plotted by the solid, the dashed, and the dotted curves. The dot-dot-dashed curve plots $g_0(Y)$.

Then using Eq. (1), the Poisson equation and the continuity equation we obtain for the wave charge density $\rho(\omega, k_x, Y)$ the integral equation

$$\frac{\omega}{k_x}\rho(\omega, k_x, Y) - \frac{2|e|cn_I}{\varepsilon B_0} g_0(Y) \int_{-\infty}^{\infty} dY' \rho(\omega, k_x, Y') R_g^{(0)}(|Y - Y'|; k_x d) = 0, \tag{3}$$

where

$$g_0(Y) = \{\frac{(1+\eta)^{-1}}{1 + Y^2/(1+\eta)^2} - \frac{1}{1+Y^2}\}, \tag{4}$$

$g_0(Y)$ is dimensionless gradient of magnetic field along y. In $R_g^{(0)}(|Y - Y'|; k_x d)$ we took into account screening of Coulomb potential by equipotential surface.

$$R_g^{(0)}(|Y - Y'|; k_x d) = K_0(|k_x d||Y - Y'|) - K_0(|k_x d|\sqrt{(Y - Y')^2 + 4}), \tag{5}$$

where $K_0(x)$ is the modified Bessel function.

From Eq. (3) it follows that its complete set of solutions can be presented as the set of symmetric solutions and the set of antisymmetric solutions. Further we will assume that $k_x d \ll 1$. Then from Eqs. (3)-(5) it follows readily that the magnetic edge waves have acoustic dispersion and their group and phase velocities have the same value. We use notation for the dimensionless wave velocity as $W = \frac{\omega}{k_x}\frac{\varepsilon B_0}{2|e|cn_I}$, given by an eigen value of the integral equation (3); its positive or negative sign corresponds to positive or negative chirality and the phase velocity. Equation (3) has infinite set of positive and negative eigen values, however, physically only a finite number of these modes, with largest $|W|$, meet assumed conditions as slower modes

have the characteristic scale of the spatial structure along y of the order of magnetic length or smaller.

To solve equation (3) numerically we introduce a new variable $X = \frac{2}{\pi}\arctan(Y)$ that changes from -1 to 1 as Y changes from $-\infty$ to ∞. Then Eq. (4) as function of X we denote also as $g_0(X)$, to simplify notations. Then the symmetric solutions of Eq. (3) obtain the form

$$\rho_s(\omega, k_x; X) = g_0(X) \sum_{k=0}^{\infty} a_{ks}^{(1)}(\omega, k_x) \left[\cos(k\pi X) - \frac{1}{2}\delta_{k,0}\right], \tag{6}$$

and they are defined by the system of linear homogeneous equations

$$W a_{ns}^{(1)} - \sum_{k=0}^{\infty} r_{n,k}^{12} a_{k,s}^{(1)} = 0. \tag{7}$$

where $n = 0, 1, 2, ...$, $\delta_{k,0}$ is the symbol Kroneckera, and the matrix elements

$$r_{n,k}^{12} = \frac{\pi}{2}\int_{-1}^{1} dX \cos(n\pi X) \int_{-1}^{1} dX' R_g^{(1)}(|\tan(\frac{\pi}{2}X) - \tan(\frac{\pi}{2}X')|, |k_x d|)$$
$$\times \left[\frac{1+\eta}{1+\eta(2+\eta)\cos^2(\pi X'/2)} - 1\right] \left[\cos(k\pi X') - \frac{1}{2}\delta_{k,0}\right]. \tag{8}$$

Point out, a similar treatment leads to pertinent equations and expressions for the antisymmetric modes density profile, $\rho_a(\omega, k_x; X)$, and their velocities. By keeping in the right hand side of Eq. (6) of the first n terms, $a_{0s}^{(1)}(\omega, k_x), ..., a_{n-1s}^{(1)}(\omega, k_x)$, and using for them the first n equations from Eqs. (7) we readily calculate the velocity of the first n MEMPs and their spatial structure. Our approach shows fast convergence.

In table 1 the velocity W for three fastest symmetric modes ($|W_{s1}| > |W_{s2}| > |W_{s3}|$) and three fastest antisymmetric modes ($|W_{a1}| > |W_{a2}| > |W_{a3}|$) are presented, within the model of $1/B(y)$ given by Eq. (2) for characteristic values of $\eta = 1$, 2

Table 1. Dimensionless wave velocity of three fastest symmetric MEMPs, W_s, and three fastest antisymmetric MEMPs, W_a.

η	W_{s1}	W_{s2}	W_{s3}	W_{a1}	W_{a2}	W_{a3}
1.0	-1.175	-0.2652	0.195 ± 0.005	-0.4190	-0.1893	0.184 ± 0.005
2.0	-1.672	-0.4028	0.247 ± 0.005	-0.6270	-0.2890	0.235 ± 0.005

Table 1 shows that the fastest mode is the fundamental symmetric MEMP which has negative chirality and velocity. The second most fast symmetric MEMP also have negative chirality and velocity for both $\eta = 1$ and 2. However, the third most fast symmetric MEMP has positive chirality (velocity) for these η. The first and the second most fast antisymmetric MEMPs have negative chirality and velocity as the third most fast antisymmetric MEMP has positive chirality and velocity for both $\eta = 1$, and 2. From table 1 it follows that the fastest symmetric MEMPs is much faster than the second fastest symmetric MEMP, $|W_{s1}|/|W_{s2}| > 4$, or the fastest antisymmetric MEMP, $|W_{s1}/|W_{a1}| \approx 2.75$. So among these modes the fastest symmetric MEMP, W_{s1}, should be manifested in experiment easier than any other MEMP as other modes are much slower and, respectively, must be much more damped.

In Figs. 2, 3 we plot charge density profiles of three fastest symmetric and antisymmetric modes for $\eta = 1$; in addition, $g_0(Y)$ is shown. It is seen that for the modes W_{s1}, W_{s2} and W_{a1},

W_{a2} with the negative chirality the wave charge density is strongly localized within the region of negative $g_0(Y)$, i.e, $-1.75 \leq Y \leq 1.75$. In addition, in Figs. 2, 3 the charge density of the MEMPs W_{s3} and W_{a3}, with the positive chirality, is more localized within the region of positive $g_0(Y)$, at $|Y| > 1.75$; notice that $\int_{-\infty}^{\infty} dY\ g_0(Y) = 0$.

We have assumed that $M_0 > 0$ and $B_{ext} > 0$. It is easy to see that the sign of chirality (velocity) of any MEMP will be changed if the sign of M_0 becomes opposite; however, it is independent of a sign of B_{ext}. If the ferromagnetic film has hysteresis then, in principle, it is possible to change a sign of M_0 while keeping the same B_{ext}. Then the chirality of a MEMP will be changed on opposite.

We have obtained that laterally inhomogeneous strong magnetic field applied to homogeneous 2DES allows "magnetic gradient" or special magnetic-edge magnetoplasmons. This mechanism is different from usual "density gradient" edge magnetoplasmons. Symmetric and antisymmetric families of magnetic-edge magnetoplasmons are obtained. The fundamental symmetric MEMP is much faster than any other MEMP and hence it should be less damped and easier to observe. The fastest MEMP is mainly localized within the region of largest (negative) magnetic gradient under the edge of magnetic film. MEMP of opposite chirality is mainly localized within the region of positive magnetic gradient that is close, but not immediately under the edge of magnetic film.

Acknowledgments

We are grateful to Lloyd W. Engel for many useful discussions on a possibility of MEMP, due to inhomogeneity of magnetic field, relevant experiments and experimental conditions. The research leading to these results has received funding from the European Union Seventh Framework Programme (FP7/2007-2013) under grant agreement nº PCOFUND-GA-2009-246542 and from the Foundation for Science and Technology of Portugal. We also acknowledge support by Brazilian FAPEAM grants: Universal Amazonas (Edital 021/2011) and PVS.

References

[1] Volkov V A and Mikhailov S A 1991 *Electrodynamics of Two-Dimensional Electron Systems in High Magnetic Fields*, in *Landau Level Spectroscopy, Modern Problems in Condensed Matter Sciences*, Ed. by G. Landwehr and E. I. Rashba (North-Holland, Amsterdam) vol 27.2 chapter 15 pp 855-907; Volkov V A and Mikhailov S A 1988 *Zh. Eksp. Teor. Fiz.* **94** 217 [1988 *Sov. Phys. JETP* **67** 1639]

[2] Kushwaha M S 2001 *Surface Science Reports* **41** pp 1-416

[3] Balev O G and Vasilopoulos P 1998 Phys. Rev. Lett. **81** 1481

[4] Khannanov M N, Fortunatov A A and Kukushkin I V 2009 *Pis'ma Zh. Eksp. Teor. Fiz.* **90** 740 [2009 *JETP Lett.* **90** 667

[5] Silva S and Balev O G 2010 *J. Appl. Phys.* **107** 104310

[6] Larkin I A and Sukhorukov E V, Phys. Rev. **49**, 5498 (1994).

[7] Jackson J D 1999 *Classical Electrodynamics* 3d ed. (John Wiley&Sons, New York)